ORGANOMETALLICS

Article

pubs.acs.org/Organometallics

Near-Infrared-Emitting Iridium(III) Complexes as Phosphorescent Dyes for Live Cell Imaging

Guoliang Zhang,[†] Huiyuan Zhang,[‡] Yuan Gao,[§] Ran Tao,[†] Lijun Xin,[†] Junyang Yi,[‡] Fuyou Li,*[,§] Wanli Liu,*[,‡,∥] and Juan Qiao*[,†]

[†]Key Lab of Organic Optoelectronics and Molecular Engineering of Ministry of Education, Department of Chemistry, Tsinghua University, Beijing 100084, People's Republic of China

[‡]MOE Key Laboratory of Protein Science, School of Life Sciences, Tsinghua University, Beijing 100084, People's Republic of China

[§]Department of Chemistry, Fudan University, Shanghai 200433, People's Republic of China

[∥]Collaborative Innovation Center for Diagnosis and Treatment of Infectious Diseases, State Key Laboratory for Diagnosis and Treatment of Infectious Diseases, The First Affiliated Hospital, College of Medicine, Zhejiang University, Hangzhou, People's Republic of China

Supporting Information

ABSTRACT: The three near-infrared-emitting cationic iridium(III) complexes $[Ir(pbq\text{-}g)_2(N^\wedge N)]^+PF_6^-$ (pbq-*g* = phenylbenzo[*g*]-quinoline; N^N = bipyridine (**1**), 1,10-phenanthroline (**2**), 4,7-diphenyl-1,10-phenanthroline (**3**)) have been demonstrated as phosphorescent dyes in live cell imaging. These complexes with different ancillary ligands show similar near-infrared (NIR) emission with $\lambda_{max,peak}$ at 698 nm and $\lambda_{max,shoulder}$ at 760 nm in CH_2Cl_2 solutions, with a moderate quantum yield of around 3%. However, these complexes behave quite differently as NIR dyes for live cell imaging. Complexes **1** and **2** exhibit exclusive staining in the cytoplasm with good cell membrane permeability under excitation at 488 nm, while **3** gives almost no cell uptake, as further determined by flow cytometry. Although the lipophilicities of these complexes follow the order **1** < **2** < **3**, their cytotoxicities are in the reverse order. The exceptionally low cytotoxicity of **3** could be attributed to its poor solubility in aqueous buffer and thus substantially low exposure dose. This comparative study suggested that the ancillary ligands could fine-tune the amphiphilicity and cytotoxicity of the cyclometalated iridium(III) complexes and thus might play a key role in the design of NIR-emitting iridium(III) complexes for practical applications in bioimaging.

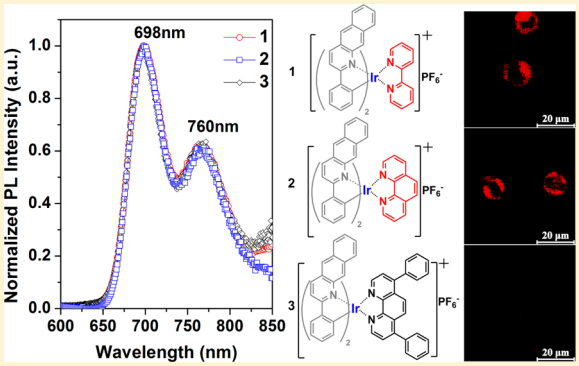

INTRODUCTION

Near-infrared (NIR) dyes have attracted increasing attention for their potential applications in optical imaging in vivo and medical diagnosis.[1−5] The diagnostic window falling in the NIR range from 650 to 900 nm surpasses the visible region and allows for bioimaging with minimal interference from tissue autofluorescence, reduced light scattering, and high tissue penetration. So far, the available NIR fluorophores for bioimaging applications are essentially limited to organic dyes, semiconductor quantum dots (QDs), and lanthanide upconversion nanophosphors.[2−5] Various organic compounds make up a major part of NIR fluorescent dyes, as for example typified by cyanines, yet many of them suffer from several significant limitations such as poor photobleaching, small Stokes shift, low detection sensitivity, etc.[2−5] The NIR QDs are relatively larger in size (10−20 nm) due to their core/shell structure and commonly contain toxic elements such as Cd and Te, which cannot be metabolized by the human body.[4,6]

Different from the aforementioned fluorophores, lanthanide and transition-metal complexes with long-lived phosphorescence and large Stokes shifts are of great current interest in the fields of chemical sensors and bioimaging.[7−12] Most of the NIR lanthanide complexes (e.g., Er, Nd, and Yb) have extremely long luminescence lifetimes (ms) due to the parity-forbidden f−f transition and unique atom spectral characteristics with relatively low quantum efficiencies.[7] In contrast, transition-metal complexes (e.g., Pt and Ir) have remarkably improved quantum yields and excellent color tunability due to strong metal-induced spin−orbit coupling.[8−13] Of particular interest are cyclometalated iridium(III) complexes, which are far more attractive as therapeutic and bioimaging reagents for cellular applications, due to the exclusively strong spin−orbit coupling of the iridium ion (coupling constant ξ_{Ir} = 3909 cm^{-1}), high quantum yield in solution, and facile and tunable excitation and emission maxima from the blue to the red region.[10−13] The cationic iridium(III) complexes show a number of superiorities: exclusive staining in the cytoplasm, low cytotoxicity, reduced

Received: July 9, 2013

   dx.doi.org/10.1021/om400676h | Organometallics XXXX, XXX, XXX−XXX

Scheme 1. Synthetic Route of the Cyclometalated Ligand pbq-*g* and Molecular Structures of the Iridium(III) Complexes

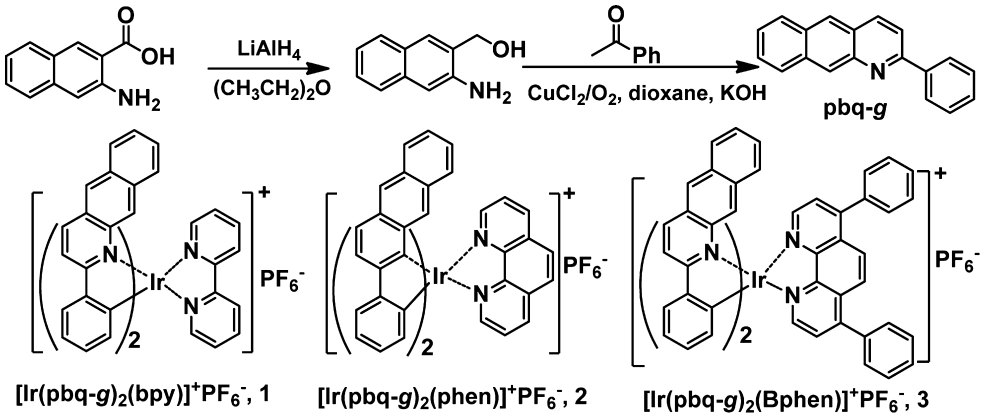

photobleaching, and good permeability of cell membranes, thus rendering iridium complexes as excellent candidates for bioimaging and cellular studies. Several groups (including our group) have reported a number of iridium(III) complexes as bioimaging regents for cellular applications.[13−16] The most commonly applied are monocationic bis-cyclometalated iridium(III) complexes with neutral N^N ligands, which can avoid the problems of low membrane permeability associated with highly charged species while still benefiting from the potential-driven preferential uptake of cations.[10−16]

However, iridium(III) complexes are underdeveloped in the NIR region[17,18] and few have been used in bioimaging. For pursuing high-efficiency NIR-emitting iridium(III) complexes, we designed phenylbenzo[*g*]quinoline (pbq-*g*) as the cyclometalated ligand and synthesized a NIR-emitting iridium(III) complex, Ir(pbq-*g*)$_2$acac, which exhibits good NIR emission with a maximum peak at 708 nm and a shoulder around 780 nm.[18] Since such a neutral complex could not be readily taken up into the cells, we further designed and synthesized three NIR-emitting cationic iridium(III) complexes with different diimine N^N ligands (Scheme 1): [Ir(pbq-*g*)$_2$(bpy)]$^+$PF$_6$ (**1**), [Ir(pbq-*g*)$_2$(phen)]$^+$ (**2**), and [Ir(pbq-*g*)$_2$(Bphen)]$^+$PF$_6^-$ (**3**). Complex **3** has been used as a NIR emitter in solution-processable organic light-emitting devices.[18b] Herein, we comparatively studied their electronic structure, photophysical and electrochemical properties, and in particular their performance as NIR dyes for live cell imaging. Because they have the same cyclometalated ligand, these three complexes exhibit very similar photophysical and electrochemical properties. Interestingly, **1** and **2** exhibited exclusive staining in the cytoplasm with good cell membrane permeability in the desirable NIR region, while **3** showed poor staining in live cells. The lipophilicity, cytotoxicity, and cellular uptake of these three complexes were further investigated.

EXPERIMENTAL SECTION

Characterization. ^{1}H NMR spectra were recorded on JEOL JNM-ECA300 (300 MHz) and JNM-ECA600 (600 MHz) NMR spectrometers with tetramethylsilane as the internal standard. Elemental analysis was performed on an Elementar Vario EL CHN elemental analyzer. Mass spectra were collected with a Thermo Electron Corp. Finnigan LTQ mass spectrometer (ESI-MS). Steady-state absorption and photoluminescence (PL) spectra were recorded with an Agilent 8453 UV−vis spectrophotometer and a Jobin Yvon fluorospectrophotometer (FluoroMax-3), respectively. The PL spectra were m-corrected, regarding the sensitivity of the detector response to emission wavelength, by using the manufacturer's procedure. PL quantum yields (Φ_{PL}) were measured in CH_2Cl_2 solutions using an absolute PL quantum yield spectrometer (C11347-11, Hamamatsu photonics k. k.).[19] The solutions were degassed by three freeze−pump−thaw cycles. PL lifetime measurements were made using a time-correlated single photon counting (TCSPC) system on a LifeSpec Red time-resolved spectrometer (Edinburgh Instruments) with a 372 nm picosecond diode laser. Cyclic voltammetry measurements were carried out on a Princeton Applied Research Model 283 potentiostat/galvanostat voltammetric analyzer in anhydrous CH_3CN solutions (10^{-3} M) at a scan rate of 200 mV/s. The supporting electrolyte was tetra-*n*-butylammonium perchlorate (0.1 M), and ferrocene was selected as the internal standard. The solution was bubbled with argon for 15 min before measurements.

Materials and Synthesis. All reactants and solvents were purchased from commercial sources and used as received unless otherwise stated. All procedures involving $IrCl_3{\cdot}xH_2O$ were carried out under an argon atmosphere.

Synthesis of 2-Phenylbenzo[*g*]quinoline (pbq-*g*). A mixture of $LiAlH_4$ (1.52 g, 40 mmol), diethyl ether (150 mL, anhydrous), and 3-amino-2-naphthoic acid (3.00 g, 16 mmol) was refluxed with stirring for 40 min. After it was cooled, the mixture was carefully quenched with deionized water (removal of excess $LiAlH_4$) and then mixed with 50 mL of NaOH solution (10%, mass fraction). The organic phase was separated, and the aqueous phase was extracted with ether three times (30 mL × 3). The combined organic phases were dried over anhydrous Na_2SO_4, filtered, and evaporated to dryness. The obtained pale yellow solid was mixed with acetophenone (2.5 mL), $CuCl_2$ (0.005 g, 0.8 mmol), dioxane (150 mL), and KOH (2.7 g, 48 mmol). Then this suspension was refluxed with stirring for 5 h under an oxygen atmosphere. After being cooled, the mixture was poured into water and extracted with dichloromethane (50 mL × 3). The combined organic phases were dried over anhydrous $MgSO_4$ and filtered, followed by concentration under vacuum. The crude residue was purified using column chromatography with petroleum ether and dichloromethane as the eluent, giving 2.7 g of the yellow desired product (yield 66%). ^{1}H NMR (600 MHz, DMSO-d_6): δ 7.94 (s, 1H), 7.84 (s, 1H), 7.82 (d, J = 8.9 Hz, 1H), 7.55 (dd, J = 7.8, 6.5 Hz, 2H), 7.39 (d, J = 7.7 Hz, 1H), 7.35 (t, J = 8.6 Hz, 2H), 6.80−6.76 (m, 4H), 6.75−6.72 (m, 1H).

Synthesis of Complexes 1 and 2. The cyclometalated iridium(III) chloro-bridged dimeric intermediate [Ir(pbq-*g*)$_2$Cl$_2$]$_2$ was prepared according to the literature methods.[18] Complexes **1** and **2** were synthesized from the reaction of the dimeric intermediate with bipyridine (bpy) and 1,10-phenanthroline (phen) as the diimine ligand, according to our previous report.[18b]

[Ir(pbq-*g*)$_2$(bpy)]$^+$PF$_6^-$ (**1**): deep orange-red solid, yield 37%. ^{1}H NMR (300 MHz, acetone-d_6): δ 8.72 (d, J = 9.2 Hz, 2H), 8.60 (dd, J = 18.2, 6.9 Hz, 6H), 8.38 (dd, J = 12.5, 8.1 Hz,4H), 8.23−8.15 (m, 2H), 8.08 (d, J = 10.9 Hz, 4H), 7.96−7.89 (m,2H), 7.58−7.50 (m, 2H), 7.43−7.35 (m, 2H), 7.23 (t, J = 7.4 Hz, 2H), 7.03 (d, J = 8.5 Hz, 2H), 6.89−6.81 (m, 2H), 6.74 (d, J = 7.9 Hz, 2H). ESI-MS (m/z): 857 [M

dx.doi.org/10.1021/om400676h | *Organometallics* XXXX, XXX, XXX−XXX

$-PF_6]^+$. Anal. Calcd for $IrC_{48}H_{32}N_4PF_6$: C, 57.54; H, 3.22; N, 5.59. Found: C, 57.35; H, 3.27; N, 5.51.

$[Ir(pbq\text{-}g)_2(phen)]^+PF_6^-$ (**2**): deep orange-red solid, yield 46%. ^1H NMR (300 MHz, acetone-d_6): δ 8.99−8.93 (m, 2H), 8.76 (d, J = 8.3 Hz, 2H), 8.63 (d, J = 9.1 Hz, 2H), 8.54 (d, J = 9.1 Hz, 2H), 8.45 (s, 2H), 8.37 (d, J = 7.5 Hz, 2H), 8.27 (dd, J = 8.2, 5.1 Hz, 2H), 7.97−7.88 (m, 6H), 7.44−7.35 (m, 2H), 7.25 (dd, J = 13.6, 6.7 Hz, 4H), 6.89−6.77 (m, 6H). ESI-MS (m/z): 881 $[M - PF_6]^+$. Anal. Calcd for $IrC_{50}H_{32}N_4PF_6$: C, 58.53; H, 3.14; N, 5.46. Found: C, 57.97; H, 3.28; N, 5.32.

Quantum Chemical Calculations. Density functional theory (DFT) and time-dependent DFT (TD-DFT) calculations on the ground and excited electronic states of the complexes were carried out at the B3LYP level.[20] "Double-ξ" quality basis sets were employed for C, H, and N (6-31G*) and Ir (LANL2DZ). A relativistic effective core potential (ECP) replaces the inner core electrons of Ir, leaving the outer core $(5s)^2(5p)^6$ electrons and the $5(d)^6$ valence electrons of Ir(III). The geometries of the singlet ground state (S_0) were fully optimized without symmetry constraints for the N−N *trans* type, which was reported as the most stable structural isomer for Ir complexes with diimine ligands.[21] The calculations were carried out with the Gaussian 03 software package using a spin-restricted formalism.[22] The electron density diagrams of molecular orbitals were obtained with the ChemBioOffice 2010 graphics program.

Confocal Luminescence Imaging of Live Cells. The 293T cell line was provided by the Institute of Biochemistry and Cell Biology, SIBS, CAS (People's Republic of China). The 293T cells were grown in MEM (modified Eagle's medium) supplemented with 10% FBS (fetal bovine serum) at 37 °C and 5% CO_2. Cells (5×10^8/L) were plated on 14 mm glass cover slips and allowed to adhere for 24 h. Before the experiments, cells were washed with PBS (phosphate buffered saline) buffer and then incubated solely with 50 μM of **1**, **2**, or **3** in DMSO/PBS (pH 7, 1/49, v/v) for 15 min at 25 °C. Cell imaging was then carried out after washing cells with PBS. Confocal luminescence imaging, including *xy*-scan, spectrum-scan and *Z*-scan luminescence imaging, was performed with an OLYMPUS IX81 laser scanning microscope and a 60× oil-immersion objective lens. Excitation of the 293T cells incubated with the Ir(III) complex was carried out with a semiconductor laser at 488 nm. Emission was collected at 690 ± 20 nm for the complex-treated 293T cells.

Cytotoxicity Assays. The in vitro cytotoxicity was measured using the Cell Counting Kit-8 assay in A20 cells. Briefly, cells growing in log phase were seeded in a 96-well flat-bottomed microplate (2×10^4 cells well^{-1}) in complete RPMI 1640 medium (GIBCO) supplemented with 10% FBS (100 μL). Complex **1**, **2**, or **3** was then added to these wells, and A20 cells were cultured with concentrations ranging from 0.1 to 100 μM in growth medium (MEM plus 10% FBS) for 30 min in triplets. After washing, these A20 cells were further cultured in growth medium without these complexes for another 24 h at 37 °C under a 5% CO_2 atmosphere. Wells containing complete medium without cells were used as blank controls. Then, 10 μL of Cell Counting Kit-8 (Dojindo, Kumamoto, Japan) was added to each well. The microplate was incubated at 37 °C under a 5% CO_2 atmosphere for another 2.5 h. The absorbance of the solutions at 450 nm referenced at 630 nm was measured with a Bio-Rad Model 680 microplate reader (Bio-Rad Laboratories, Hercules, CA). The viability of cell growth was calculated using a reported formula.[16a] The results were given as mean ± SEM over three independent experiments. The IC_{50} values of the complexes were determined from the dose dependence of surviving cells after the 24 h culture.

Flow Cytometry. A20 cells were cultured in complete RPMI 1640 medium (GIBCO) supplemented with 10% FBS. The culture medium was removed by centrifuge, and 1×10^6 cells were suspended in 100 μL of PBS−DMSO (49/1, v/v) containing complex **1**, **2**, or **3** at concentrations of 0, 0.1, 1, 10, and 100 μM, respectively. After an incubation time of 15 min, the cells were washed three times by PBS. Samples were analyzed by a LSR II flow cytometer (Becton, Dickinson and Co., Franklin Lakes, NJ, USA) with excitation at 488 nm and emission at 690 nm. The number of cells analyzed for each sample was between 30000 and 40000.

Measurement of Lipophilicity. The lipophilicity is referred to as log $P_{o/w}$ (where $P_{o/w}$ = octanol/water partition coefficient). The lipophilicity of these complexes has been determined by a classical method which is called the shake-flask method.[23] Equal amounts of *n*-octanol and PBS were completely mixed by an oscillator for 24 h. The mixture was then left to separate for another 24 h to finally yield water and octanol phases, each saturated with the other. Then the oil and water layers were separated with a separating funnel. Each complex was carefully dissolved in octanol saturated with PBS (the concentration corresponded to c_a). Then it was mixed with equal amounts of PBS saturated with octanol and shaken again as described above. After separation, the final concentrations of compounds in octanol corresponded to c_o. In addition, c_0 was measured by UV−vis spectrophotometry at λ 490 nm, and the partition coefficient ($P_{o/w}$) for each complex was calculated by the equation

$$P_{o/w} = c_o/(c_a - c_o)$$

RESULTS AND DISCUSSION

Synthesis of the Ir(III) Complexes. The three cationic iridium(III) complexes are obtained in moderate yields via treatment of the chloro-bridged dimer precursor with the corresponding ancillary ligands, followed by a counterion exchange reaction from Cl^- to PF_6^-. In a previous report,[18] the cyclometalated ligand pbq-*g* was prepared from the Friedländer condensation of 3-amino-2-naphthaldehyde with acetophenone in a six-step scheme with low total yield. Here, we report a high yield and convenient synthetic route starting with the same reagent (Scheme 1). 3-Amino-2-naphthoic acid is first reduced by $LiAlH_4$ to give a hybrid of 3-amino-2-naphthaldehyde and 3-amino-2-naphthalenemethanol. Without further purification, this mixture was oxidatively coupled and cyclized with ketones as well as aldehydes in the presence of a copper catalyst and a base to afford benzoquinoline in a good yield of 75%.[24]

Photophysical Properties. The UV−vis absorption and photoluminescence (PL) spectra of these complexes were obtained in degassed CH_2Cl_2 solutions at room temperature. As shown in Figure 1, these three complexes exhibit similar absorption peaks from 300 to 600 nm. The intense absorption bands below 350 nm could be assigned to spin-allowed intraligand $\pi \rightarrow \pi^*$ transitions, while the relatively weak bands above 350 nm correspond to mixed transitions of ^{1}MLCT and ^{3}MLCT (singlet and triplet metal to ligand charge transfer) with LLCT (ligand to ligand charge transfer). These complexes

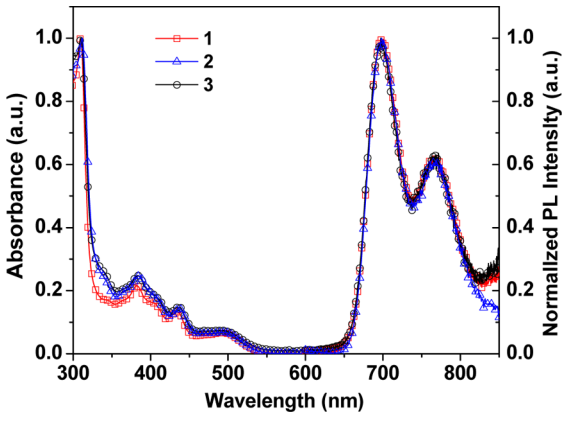

Figure 1. Room-temperature absorption (left) and photoluminescence (PL) spectra (right, corrected to 850 nm corresponding to the instrument limit) of complexes **1**−**3** in degassed CH_2Cl_2 solutions. The excitation wavelength was 436 nm.

dx.doi.org/10.1021/om400676h | *Organometallics* XXXX, XXX, XXX−XXX

Table 1. Photophysical and Electrochemical Characteristics of Complexes 1−3

		room temp emission[b]					electrochemical data[c]		
	absorption[a] λ (nm) (ε ($\times 10^4$ M^{-1} cm^{-1}))	λ (nm)	τ (μs)	Φ_{PL} (%)	$k_r \times 10^4$	$k_{nr} \times 10^4$	$E_{ox}^{1/2}$ (V)	$E_{red}^{1/2}$ (V)	E_g (eV)[d]
1	310 (8.4), 382 (1.8), 433 (1.1), 493 (0.6)	698, 760	2.1	2.9	1.4	46	1.00	−1.60, −1.79	2.60
2	310 (9.8), 386(2.5), 438(1.4), 490(0.8)	698, 760	1.2 (34%), 3.0 (66%)	3.3			0.97	−1.61, −1.79	2.57
3[18b]	309 (7.7), 383 (1.9), 436 (1.1), 493 (0.5)	698, 760	1.86	3.5	1.9	52	0.99	−1.60, −1.74	2.60

[a]In CH_2Cl_2 solutions (10 μM). ε denotes the molar extinction coefficients. [b]In degassed CH_2Cl_2 (1×10^{-5} M) solutions. Φ_{PL} was measured using an absolute PL quantum yield measurement system. [c]Collected in CH_3CN solutions (10^{-3} M). The data are versus Fc^+/Fc (Fc is ferrocene). [d]$E_g = E_{ox}^{1/2} - E_{red}^{1/2}$.

also show almost identical emission bands, with a maximum peak at 698 nm and a shoulder around 760 nm. However, complexes **2** and **3** bear slightly higher absorption intensity and stronger luminescent emission than **1** does. Of note, the PL spectra were corrected to the apparatus response to eliminate the spectra-response characteristics (see Figure S1 in the Supporting Information for the noncorrected spectra). The corrected PL spectra show slightly red-shifted emission bands (4−8 nm) and remarkably stronger shoulder peaks in comparison to the noncorrected spectra. Table 1 gives the detailed photophysical properties of these complexes in degassed CH_2Cl_2 solutions. Complex **3** has a slightly shorter PL lifetime of 1.86 μs in comparison to **1** that contributes to a slightly higher quantum yield (Φ_{PL}: 2.9% of **1** vs 3.5% of **3**). Likewise, **3** has a slightly greater solution phase radiative decay rate (k_r) and nonradiative rate (k_{nr}). For complex **2**, the Φ_{PL} value is 3.3%, just between that of **1** and **3**, and the excited-state lifetime exhibits a biexponential characteristic. Since the PL decay characteristics are not single exponential, k_r and k_{nr} are not estimated. The underlying reason is currently unknown and needs further investigation.

When they are dissolved in aerated PBS/DMSO (pH 7, 49/1, v/v) buffer, however, these complexes behave differently. Complexes **1** and **2** have fair solubility in the buffer and still show moderate NIR emission; however, **3** has poor solubility and easily precipitates, thus giving nearly no emission in this buffer. These facts are mainly attributed to the high hydrophobicity of the ligand Bphen with the two phenyl rings on the 1,10-phenanthroline unit. For complexes **1** and **2**, the emission profile was retained in the aerated PBS/DMSO buffer (Figure S2 in the Supporting Information), whereas the Φ_{em} values was significantly reduced to 0.1% because of quenching from oxygen and aggregation.

Electrochemical Properties. The electrochemical properties were studied by cyclic voltammetry using ferrocene as a reference standard. The cyclic voltammograms are displayed in Figure 2, and the electrochemical data are given in Table 1. In anhydrous CH_3CN solutions, these three complexes also show similar electrochemical characteristics with two reversible reduction processes and one reversible oxidation process. Two reversible reduction processes arose at half-wave potentials of −1.60 and −1.79 V for **1**, −1.61 and −1.79 V for **2**, and −1.60 and −1.74 V for **3** (Figure 2). The reversible oxidation process occurred at half-wave potentials of 1.00 V for **1**, 0.97 V for **2**, and 0.99 V for **3**. As the differences in data among the three complexes are within the range of experimental error, we may safely draw the conclusion that the ancillary ligands have a very limited effect on the electronic structures of these complexes.

Theoretical Calculations. To further shed light on the photophysical and electrochemical characteristics of these

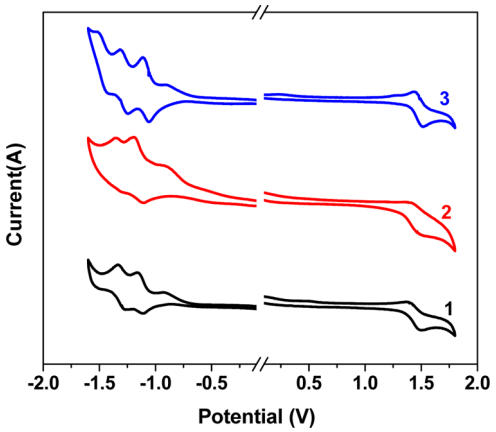

Figure 2. Cyclic voltammograms of complexes **1**−**3** in anhydrous CH_3CN solutions (10^{-3} M).

complexes, theoretical studies of electronic structures were carried out using density functional theory. These three complexes exhibit very similar HOMO and LUMO configurations. As shown in Figure 3, the HOMO orbital primarily

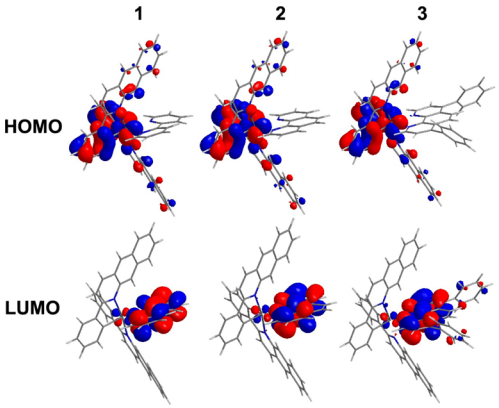

Figure 3. Isodensity plots of the frontier orbitals of $Ir(pbq\text{-}g)_2(bpy)]^+PF_6^-$ (**1**), $Ir(pbq\text{-}g)_2(phen)]^+PF_6^-$ (**2**), and $[Ir(pbq\text{-}g)_2(Bphen)]^+PF_6^-$ (**3**). All of the MO surfaces correspond to an isocontour value of $|\Psi| = 0.03$.

resides on the iridium center and the phenyl groups of the cyclometalated ligands pbq-*g*, while the LUMO is dominantly located on the N^N ancillary ligands. For complex **3**, the attached noncoplanar phenyls in bphen make a negligible contribution to the LUMOs. The vertical excitation energies and molecular orbitals involved in the excitations for the first two triplets are summarized in Table 2. The calculated $T_1 \rightarrow S_0$ transition energies are almost the same (692−694 nm), which are very close to the experimentally observed peaks at 698 nm.

dx.doi.org/10.1021/om400676h | Organometallics XXXX, XXX, XXX−XXX

Table 2. First Two Triplet States for the Complexes Calculated from the TD-DFT Approach

	state (E (eV), λ (nm))[a]	dominant excitation[b]	character
1	T_1 (1.787, 694)	H-1 → L+1 (0.46)	d_π(Ir)−π(pbq-g) → π^*(pbq-g)
		H-2 → L+2 (0.32)	d_π(Ir)−π(pbq-g) → π^*(pbq-g)
	T_2 (1.790, 693)	H-1 → L+2 (0.47)	d_π(Ir)−π(pbq-g) → π^*(pbq-g)
		H-2 → L+1 (0.32)	d_π(Ir)−π(pbq-g) → π^*(pbq-g)
2	T_1 (1.784, 695)	H-1 → L+3 (0.33)	d_π(Ir)−π(pbq-g) → π^*(pbq-g) /π^*(phen)
		H-2 → L+2 (0.32)	d_π(Ir)−π(pbq-g) → π^*(pbq-g)
	T_2 (1.786, 694)	H-2 → L+3 (0.23)	d_π(Ir)−π(pbq-g) →π^*(pbq-g)/ π^*(phen)
		H-1 → L+2 (0.47)	d_π(Ir)−π(pbq-g) → π^*(pbq-g)
3[18b]	T_1 (1.789, 693)	H-2 → L+2 (0.24)	d_π(Ir)−π(pbq-g) → π^*(pbq-g)
		H-1 → L+3 (0.20)	d_π(Ir)−π(pbq-g) →π^*(pbq-g)/ π^*(Bphen)
	T_2 (1.791, 692)	H-1 → L+2 (0.32)	d_π(Ir)−π(pbq-g) → π^*(pbq-g)
		H-2 → L+3 (0.15)	d_π(Ir)−π(pbq-g) →π^*(pbq-g) /π^*(Bphen)

[a]Data in parentheses are excitation energies and corresponding wavelengths. [b]H and L denote the HOMO and LUMO, respectively; data in parentheses are the contributions of corresponding excitations.

However, the electron transition is not from pure HOMO to LUMO but from HOMO-1 and HOMO-2 to LUMO+1 or other orbitals because of the selection rule of the spectrum. These transitions have multiconfigurational character. For complex **1**, the T_1 and T_2 states both have predominantly mixed ^{3}MLCT ($d\pi$(Ir) → $\pi^*_{C\hat{}N}$) and ^{3}LC ($\pi_{C\hat{}N}$ → $\pi^*_{C\hat{}N}$) characters. However, for **2** and **3**, there is some contribution from ^{3}MLCT ($d\pi$(Ir) → $\pi^*_{N\hat{}N}$) and ^{3}LLCT ($\pi^*_{C\hat{}N}$ → $\pi^*_{N\hat{}N}$) in addition to ^{3}MLCT ($d\pi$(Ir) → $\pi^*_{C\hat{}N}$) and ^{3}LC ($\pi_{C\hat{}N}$ → $\pi^*_{C\hat{}N}$) transitions.

Lipophilicity. The lipophilicity is a key character to estimate the ability of a cellular probe to permeate biological membranes.[25] It is commonly referred to as log $P_{o/w}$, where $P_{o/w}$ is the partition coefficient of the compound in n-octanol/water. In this work, the log $P_{o/w}$ values of these three complexes were readily determined by the shake-flask method.[23] Complexes **1** and **2** showed comparable lipophilicity, with log $P_{o/w}$ values of 0.13 and 0.18, respectively. In comparison, **3** had the largest log $P_{o/w}$ value of 0.88, which could be attributed to the significantly enhanced hydrophobic nature of the Bphen ligand with the two phenyl rings on the 1,10-phenanthroline unit. Overall, the lipophilicity follows the order **1** < **2** < **3**, which is consistent with the lipophilicity of the ancillary diimine ligands (bpy < phen < Bphen).[14e]

Cytotoxicity. Cytotoxicity is often a concern in cellular imaging studies. Recently, Lo et al. comparatively examined the cytotoxic effect of Ir(III) polypyridine complexes toward Hela cells and found that the complexes with bphen as the ancillary ligands had slightly higher cytotoxicity than the counterparts with bipyridine (bpy) due to an increase of the lipophilicity of the diimines.[14e] The cytotoxic effect of these three NIR-emitting complexes was examined using a Cell Counting Kit-8 toward A20 cells after exposure to each complex for 30 min, which is a typical incubation time in cell staining experiments. As shown in Figure 4, it is clear that complex **1** with bpy as the ancillary ligand showed significantly higher cytotoxicity than **2**

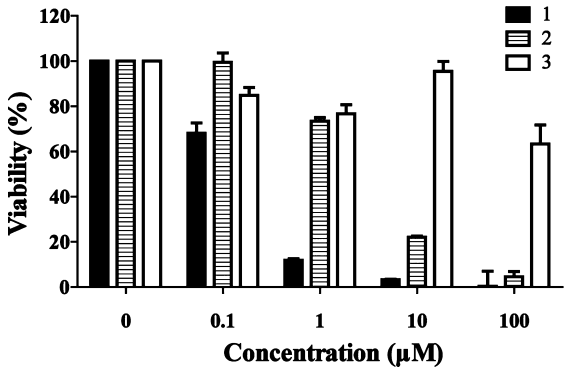

Figure 4. Cell viability values (%) estimated using a Cell Counting Kit-8 on A20 cells versus the concentrations of each complex after incubation at 37 °C for 30 min. These A20 cells after washing off the non-uptaken complex were continued to be cultured at 37 °C for 24 h.

and **3** with phen and Bphen as the ancillary ligands, respectively. Complex **1** killed over 80% of A20 cells at a concentration of 1 μM, while complexes **2** and **3** only killed around 20%. Per our calculation, the IC_{50} value of **1** was 0.19 ± 0.03 μM (mean ± SEM). In contrast, **3** never showed such high cytotoxicity even at a concentration of 100 μM. It is noteworthy that the cytotoxicity of **2** is just between those of **1** and **3**. Its IC_{50} value was about 2.85 ± 0.04 μM, which is 15 times higher than that of **1**. Although the lipophilicity of these complexes follows the order **1**< **2** < **3**, their cytotoxicity is obviously in the order **1** > **2** > **3**. Complex **3** with the highest lipophilicity exhibited the lowest cytotoxicity among these three complexes. These results seem to be different from the observation of Lo et al. that the Ir(III) polypyridine complexes with an ancillary ligand of higher lipophilicity are more cytotoxic.[14e] It is our speculation that these inconsistencies might be reconciled by the large differences of these three complexes in terms of their lipophilicity and the subsequent solubility at neutral pH in an aqueous buffer. The higher cytotoxicity of **1** and **2** could mainly be ascribed to its relatively good lipophilicity of the particularly large cyclometalated ligands for NIR emission.[14a,c,23] The cytotoxic problems of **1** and **2** can be avoided by employing a low dose of the complex with a short incubation time with the cells. For complex **3**, the exceptionally low cytotoxicity could be simply due to its poor solubility and thus the substantially low exposure dose. In the experiments, we found that complex **3** frequently showed an aggregation or precipitation phenomenon, suggesting poor solubility at neutral pH in aqueous buffer at a concentration higher than 100 μM; thus, no higher concentration was tested further in this cytotoxicity experiment. The highest lipophilicity of **3** likely makes it poorly soluble at neutral pH in aqueous buffer in comparison to **1** and **2** with less lipophilicity. Because of these features, it is intriguing to compare the capability of these three complexes in live cell staining and uptake experiments.

Luminescent Imaging of the Complex-Treated Cells. The practical application of these three complexes in luminescence imaging of living 293T cells was investigated by employing a confocal laser scanning microscope. 293T cells showed negligible background fluorescence. After incubation with 50 μM complex **1** or **2** in DMSO/PBS (pH 7, 1/49, v/v) for 15 min at 25 °C, intense intracellular luminescence with a

dx.doi.org/10.1021/om400676h | Organometallics XXXX, XXX, XXX–XXX

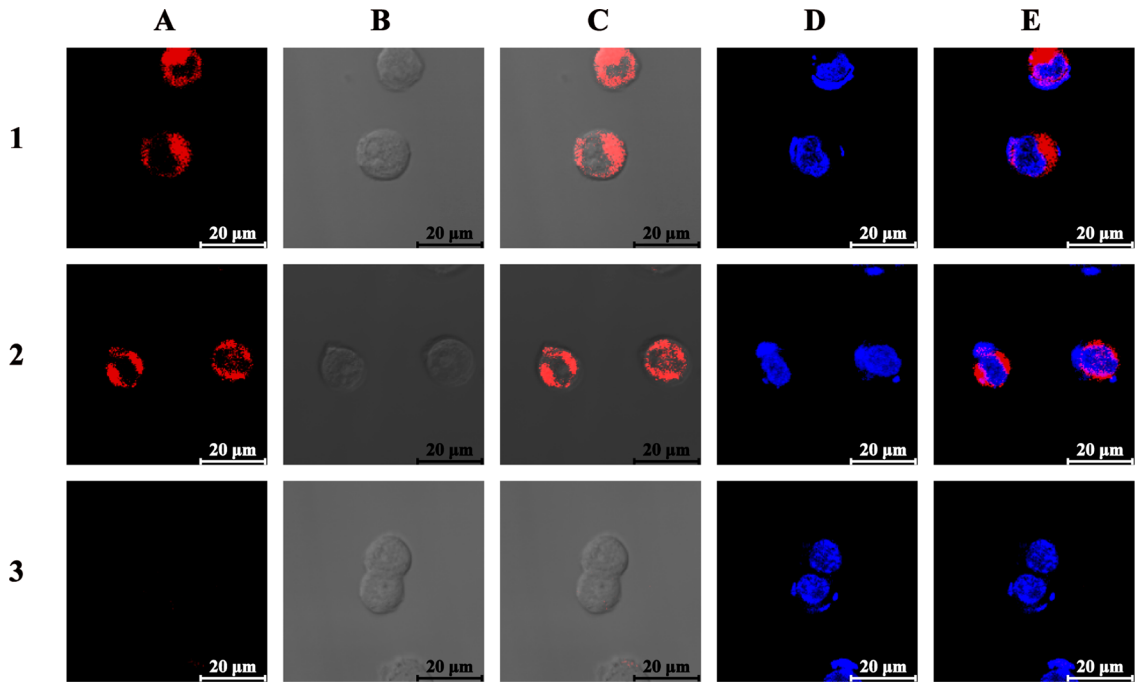

Figure 5. Confocal luminescence images of living 293T cells incubated with 50 μM complex **1** or **2** and 5 μM complex **3** in DMSO/PBS (pH 7, 1/49, v/v) for 15 min at 25 °C and then further treatment with Hochest 33258: (A) confocal luminescence images of the complexes (λ_{ex} 488 nm, λ_{em} 690 ± 20 nm); (B) bright-field images; (C) overlay of panels A and B; (D) confocal fluorescent images of Hochest 33258 (λ_{ex} 350 nm, λ_{em} 460 ± 20 nm); (E) overlay of panels A and D.

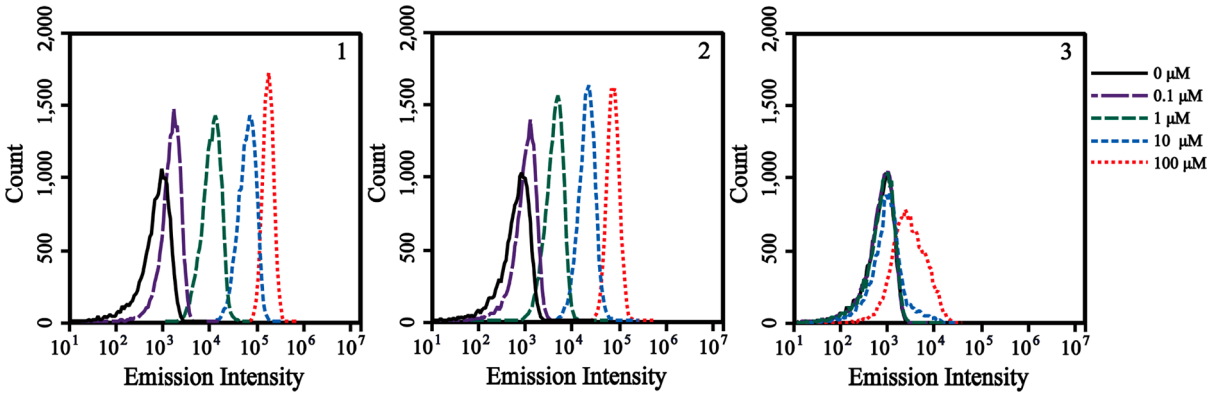

Figure 6. Flow cytometric results of A20 cells incubated with complex **1**, **2**, or **3** at concentrations of 0, 0.1, 1, 10, and 100 μM, respectively.

high signal to noise ratio (>20) was observed (Figure 5), peaking at 690 nm. Differential interference contrast (DIC) bright-field measurements after treatment with **1** or **2** demonstrated that the cells were viable throughout the imaging experiments. Furthermore, we performed the costaining experiments of the cells with the complex and another commercial nucleus-staining Hochest 33258 (blue emission). As shown in Figure 5, complexes **1** and **2** were internalized into the cells and were evident in the cytoplasm over the nucleus and membrane. That is, **1** and **2** were internalized into the cells rather than merely staining the membrane surface. Even when the dose was decreased to 5 μM, complexes **1** and **2** also showed their exclusive staining in the cytoplasm (Figure S3 in the Supporting Information).

Considering the relatively poor solubility of complex **3** in DMSO/PBS buffer, 293T cells were treated with **3** at a low concentration of 5 μM by the same procedure. Unfortunately, no intracellular luminescence was observed (Figure 5). Increasing the dose to 50 μM and elongating the incubation time to 30 min did not improve the staining (Figure S3 in the Supporting Information). As discussed above, that is mainly due to the relatively poor solubility and high lipophilicity of **3** in DMSO/PBS buffer.

Flow Cytometry. The cellular uptake characteristics of these three complexes were further studied by flow cytometry on A20 cells. Under excitation at 488 nm, the cell samples loaded with complex **1** or **2**, even at a concentration as low as 0.1 μM, exhibited higher emission intensities in comparison to the autofluorescence of untreated A20 cells (Figure 6). With an increase in the concentration, the emission intensity of the cells was significantly enhanced in a dose-dependent manner. In contrast, all of the cells loaded with **3** did not give discernible emission at a concentration from 0.1 to 10 μM. Only when the concentration was increased up to 100 μM was distinct emission detected from the cells. Of note, at this concentration, complex **3** frequently showed aggregation or precipitation

dx.doi.org/10.1021/om400676h | *Organometallics* XXXX, XXX, XXX–XXX

phenomena. These results clearly indicate that complexes **1** and **2** can be efficiently internalized by the cells, while **3** has very poor cell uptake efficiency, which agrees well with the results of live cell imaging experiments.

CONCLUSIONS

To conclude, we have demonstrated three NIR-emitting cationic iridium(III) complexes with a maximum peak at 698 nm and a shoulder around 760 nm as phosphorescent dyes for live cell imaging. Though the variation of diimine ancillary ligands has little influence on the photophysical properties in organic solvents of the corresponding complexes, they are fundamental to cellular uptake and bioimaging in view of solubility, lipophilicity, and cytotoxicity in aqueous buffer. $[Ir(pbq\text{-}g)_2(phen)]^+PF_6^-$ (**2**), with relatively low cytotoxicity, is a promising NIR dye based on an iridium(III) complex for exclusive luminescence staining in the cytoplasm of live cells. An ongoing challenge is the design of NIR-emitting iridium(III) complexes with high luminescence quantum yields and desirable biocompatibility, including high amphiphilicity and low cytotoxicity.

ASSOCIATED CONTENT

Supporting Information

Figures and tables giving noncorrected photoluminescent (PL) spectra of these three complexes in CH_2Cl_2 solutions, PL spectra of complexes **1** and **2** in DMSO/PBS (pH 7, 1/49, v/v) at 25 °C, confocal images of 293T cells incubated with 5 μM complex **1** or **2** and 50 μM complex **3** in DMSO/PBS (pH 7, 1/49, v/v) at 25 °C for 15 min, and optimized geometries of complexes **1**−**3** in *xyz* format. This material is available free of charge via the Internet at http://pubs.acs.org.

AUTHOR INFORMATION

Corresponding Author

*E-mail: qjuan@mail.tsinghua.edu.cn (J.Q.); fyli@fudan.edu.cn (F.L.); liulab@tsinghua.edu.cn (W.L.).

Notes

The authors declare no competing financial interest.

ACKNOWLEDGMENTS

We thank the National Nature Science Foundation of China (No. 51073089 and 21161160447) and the National Key Basic Research and Development Program of China (No. 2011CB808403) for financial support.

REFERENCES

(1) (a) Weissleder, R. *Nat. Biotechnol.* **2001**, *19*, 316. (b) Frangioni, J. V. *Curr. Opin. Chem. Biol.* **2003**, *7*, 626.

(2) (a) Kobayashi, H.; Ogawa, M.; Alford, R.; Choyke, P. L.; Urano, Y. *Chem. Soc. Rev.* **2010**, *110*, 2620. (b) Hilderbrand, S. A.; Weissleder, R. *Curr. Opin. Chem. Biol.* **2010**, *14*, 71.

(3) (a) Yuan, L.; Lin, W.; Zheng, K.; He, L.; Huang, W. *Chem. Soc. Rev.* **2013**, *42*, 622. (b) Escobedo, J. O.; Rusin, O.; Lim, S.; Strongin, R. M. *Curr. Opin. Chem. Biol.* **2010**, *14*, 64. (c) Qian, G.; Wang, Z. Y. *Chem. Asian J.* **2010**, *5*, 1006.

(4) (a) Aswathy, R. G.; Yoshida, Y.; Maekawa, T.; Kumar, D. S. *Anal. Bioanal. Chem.* **2010**, *397*, 1417. (b) Wang, C.; Gao, X.; Su, X. *Anal. Bioanal. Chem.* **2010**, *397*, 1397. (c) Selvan, S. T.; Tan, T. T. Y.; Yi, D. K.; Jana, N. R. *Langmuir* **2010**, *26* (14), 11631. (d) Ma, Q.; Su, X. *Analyst* **2010**, *135*, 1867.

(5) Zhou, J.; Liu, Z.; Li, F. Y. *Chem. Soc. Rev.* **2012**, *41*, 1323.

(6) Choi, H. S.; Frangioni, J. V. *Mol. Imaging* **2010**, *9*, 291.

(7) (a) Eliseeva, S. V.; Bűnzli, J. C. G. *Chem. Soc. Rev.* **2010**, *39*, 189. (b) Montgomery, C. P.; Murray, B. S.; New, E. J.; Pal, R.; Parker, D. *Acc. Chem. Res.* **2009**, *42*, 925. (c) New, E. J.; Congreve, A.; Parker, D. *Chem. Sci.* **2010**, *1*, 111. (d) Bünzli, J. C. G. *Chem. Rev.* **2010**, *110*, 2729.

(8) (a) Zhao, Q.; Huang, C. H.; Li, F. Y. *Chem. Soc. Rev.* **2011**, *40*, 2508. (b) Zhao, Q.; Li, F. Y.; Huang, C. H. *Chem. Soc. Rev.* **2010**, *39*, 3007.

(9) Ma, D. L.; Ma, V. P. Y.; Chan, D. S. H.; Leung, C. H. *Coord. Chem. Rev.* **2012**, *256*, 3087.

(10) Fernández-Moreira, V.; Thorp-Greenwood, F. L.; Coogan, M. P. *Chem. Commun.* **2010**, *46*, 186.

(11) Lo, K. K.-W.; Choi, A. W.-T.; Law, W. H.-T. *Dalton Trans.* **2012**, *41*, 6021.

(12) Lo, K. K.-W.; Zhang, K. Y. *RSC Adv.* **2012**, *2*, 12069.

(13) (a) Yu, M.; Zhao, Q.; Shi, L.; Li, F. Y.; Zhou, Z.; Yang, H.; Yi, T.; Huang, C. H. *Chem. Commun.* **2008**, 2115. (b) Zhao, Q.; Yu, M.; Shi, L.; Liu, S.; Li, C.; Shi, M.; Zhou, Z.; Huang, C. H.; Li, F. Y. *Organometallics* **2010**, *29*, 1085. (c) Xiong, L.; Zhao, Q.; Chen, H.; Wu, Y.; Dong, Z.; Zhou, Z.; Li, F. Y. *Inorg. Chem.* **2010**, *49*, 6402. (d) Li, C.; Yu, M.; Sun, Y.; Wu, Y.; Huang, C. H.; Li, F. Y. *J. Am. Chem. Soc.* **2011**, *133*, 11231. (e) Wu, H.; Yang, T.; Zhao, Q.; Zhou, J.; Li, C.; Li, F. Y. *Dalton Trans.* **2011**, *40*, 1969. (f) Wu, Y. Q.; Jing, H.; Dong, Z. S.; Zhao, Q.; Wu, H. Z.; Li, F. Y. *Inorg. Chem.* **2011**, *50*, 7412. (g) Yang, T. S.; Liu, Q.; Pu, S. Z.; Dong, Z. S.; Huang, C. H.; Li, F. Y. *Nano Res.* **2012**, *5*, 494. (h) Li, C. Y.; Liu, Y.; Wu, Y. Q.; Sun, Y.; Li, F. Y. *Biomaterials* **2013**, *34*, 1223.

(14) (a) Lo, K. K.-W.; Lee, P.-K.; Lau, J. S.-Y. *Organometallics* **2008**, *27*, 2998. (b) Lau, J. S.-Y.; Lee, P.-K.; Tsang, K. H.-K.; Ng, C. H.-C.; Lam, Y.-W.; Cheng, S.-H.; Lo, K. K.-W. *Inorg. Chem.* **2009**, *48*, 708. (c) Zhang, K. Y.; Lo, K. K.-W. *Inorg. Chem.* **2009**, *48*, 6011. (d) Zhang, K. Y.; Li, S. P.-Y.; Zhu, N.; Or, I. W.-S.; Cheung, M. S.-H.; Lam, Y.-W.; Lo, K. K.-W. *Inorg. Chem.* **2010**, *49*, 2530. (e) Lee, P.-K.; Liu, H.-W.; Yiu, S.-M.; Louie, M.-W.; Lo, K. K.-W. *Dalton Trans.* **2011**, *40*, 2180. (f) Li, S. P. Y.; Tang, T. S. M.; Yiu, K. S. M.; Lo, K. K. W. *Chem. Eur. J.* **2012**, *18*, 13342. (g) Lo, K. K. W.; Chan, B. T. N.; Liu, H. W.; Zhang, K. Y.; Li, S. P. Y.; Tang, T. S. M. *Chem. Commun.* **2013**, *49*, 4271.

(15) (a) Ma, D.-L.; Wong, W.-L.; Chung, W.-H.; Chan, F.-Y.; So, P.-K.; Lai, T.-S.; Zhou, Z.-Y.; Leung, Y.-C.; Wong, K.-Y. *Angew. Chem., Int. Ed.* **2008**, *47*, 3735. (b) Ho, C.-L.; Wong, K.-L.; Kong, H.-K.; Ho, Y.-M.; Chan, C. T.-L.; Kwok, W.-M.; Leung, K. S.-Y.; Tam, H.-L.; Lam, M. H.-W.; Ren, X.-F.; Ren, A.-M.; Feng, J.-K.; Wong, W.-Y. *Chem. Commun.* **2012**, *48*, 2525. (c) Ma, D. L.; Zhong, H. J.; Fu, W. C.; Chan, D. S. H.; Kwan, H. Y.; Fong, W. F.; Chung, L. H.; Wong, C. Y.; Leung, C. H. *PLoS One* **2013**, *8*, e55751.

(16) (a) Liu, X. M.; Liu, S. J.; Long, Q.; Ma, Y.; Yang, H. R.; Wang, J. X.; Zhai, Z.; Lin, Y. F.; Li, H. R.; He, J. H.; Zhao, Q.; Li, F. Y.; Huang, W. *J. Mater. Chem.* **2012**, *22*, 7894. (b) Ma, Y.; Liu, S. J.; Wu, Y. Q.; Yang, H. R.; Yang, C. J.; Zhao, Q.; Wu, H. Z.; Liu, X. M.; Li, F. Y.; Huang, W. *J. Mater. Chem.* **2011**, *21*, 18974.

(17) (a) Chen, H. Y.; Yang, C. H.; Chi, Y.; Cheng, Y. M.; Yeh, Y. S.; Chou, P. T.; Hsieh, H. Y.; Liu, C. S.; Peng, S. M.; Lee, G. H. *Can. J. Chem.* **2006**, *84*, 309. (b) Williams, E. L.; Li, J.; Jabbour, G. E. *Appl. Phys. Lett.* **2006**, *89*, 083506. (c) Yi, C.; Yang, C. J.; Liu, J.; Xu, M.; Wang, J. H.; Cao, Q. Y.; Gao, X. C. *Inorg. Chim. Acta* **2007**, *360*, 3493. (d) Palmer, J. H.; Durrell, A. C.; Gross, Z.; Winkler, J. R.; Gray, H. B. *J. Am. Chem. Soc.* **2010**, *132*, 9230. (e) Koren, K.; Borisov, S. M.; Saf, R.; Klimant, I. *Eur. J. Inorg. Chem.* **2011**, 1531. (f) Palmer, J. H.; Brock-Nannestad, T.; Mahammed, A.; Durrell, A. C.; VanderVelde, D.; Virgil, S.; Gross, Z.; Gray, H. B. *Angew. Chem., Int. Ed.* **2011**, *50*, 9433.

(18) (a) Qiao, J.; Duan, L.; Tang, L. T.; He, L.; Wang, L. D.; Qiu, Y. *J. Mater. Chem.* **2009**, *19*, 6573. (b) Tao, R.; Qiao, J.; Zhang, G. L.; Duan, L.; Wang, L. D.; Qiu, Y. *J. Phys. Chem. C* **2012**, *116*, 11658. (c) Tao, R.; Qiao, J.; Zhang, G. L.; Duan, L.; Chen, C.; Wang, L. D.; Qiu, Y. *J. Mater. Chem. C* **2013**, *1*, 6446.

(19) Endo, A.; Suzuki, K.; Yoshihara, T.; Tobita, S.; Yahiro, M.; Adachi, C. *Chem. Phys. Lett.* **2008**, *460*, 155.

(20) (a) Lee, C. T.; Yang, W. T.; Parr, R. G. *Phys. Rev. B* **1988**, *37*, 785. (b) Becke, A. D. *J. Chem. Phys.* **1993**, *98*, 5648.

(21) He, L.; Qiao, J.; Duan, L.; Dong, G. F.; Zhang, D. Q.; Wang, L. D.; Qiu, Y. *Adv. Funct. Mater.* **2009**, *19*, 2950.
(22) Frisch, M. J.; Trucks, G. W.; Schlegel, H. B.; Scuseria, G. E.; Robb, M. A.; Cheeseman, J. R.; Montgomery, J. A., Jr.; Vreven, T.; Kudin, K. N.; Burant, J. C.; Millam, J. M.; Iyengar, S. S.; Tomasi, J.; Barone, V.; Mennucci, B.; Cossi, M.; Scalmani, G.; Rega, N.; Petersson, G. A.; Nakatsuji, H.; Hada, M.; Ehara, M.; Toyota, K.; Fukuda, R.; Hasegawa, J.; Ishida, M.; Nakajima, T.; Honda, Y.; Kitao, O.; Nakai, H.; Klene, M.; Li, X.; Knox, J. E.; Hratchian, H. P.; Cross, J. B.; Bakken, V.; Adamo, C.; Jaramillo, J.; Gomperts, R.; Stratmann, R. E.; Yazyev, O.; Austin, A. J.; Cammi, R.; Pomelli, C.; Ochterski, J. W.; Ayala, P. Y.; Morokuma, K.; Voth, G. A.; Salvador, P.; Dannenberg, J. J.; Zakrzewski, V. G.; Dapprich, S.; Daniels, A. D.; Strain, M. C.; Farkas, O.; Malick, D. K.; Rabuck, A. D.; Raghavachari, K.; Foresman, J. B.; Ortiz, J. V.; Cui, Q.; Baboul, A. G.; Clifford, S.; Cioslowski, J.; Stefanov, B. B.; Liu, G.; Liashenko, A.; Piskorz, P.; Komaromi, I.; Martin, R. L.; Fox, D. J.; Keith, T.; Al-Laham, M. A.; Peng, C. Y.; Nanayakkara, A.; Challacombe, M.; Gill, P. M. W.; Johnson, B.; Chen, W.; Wong, M. W.; Gonzalez, C.; Pople, J. A. *Gaussian 03*; Gaussian, Inc., Wallingford, CT, 2004.
(23) Jiang, W. L.; Gao, Y.; Sun, Y.; Ding, F.; Xu, Y.; Bian, Z. Q.; Li, F. Y.; Bian, J.; Huang, C. H. *Inorg. Chem.* **2010**, *49*, 3252.
(24) Cho, C. S.; Ren, W. X.; Shim, S. C. *Tetrahedron Lett.* **2006**, *47*, 6781.
(25) VanBrocklin, H. F.; Liu, A.; Welch, M. J.; O'Neil, J. P.; Katzenellenbogen, J. A. *Steroids* **1994**, *59*, 34.